

Flow Properties of Polystyrene Solutions Under High Shear Rates

A. H. ABDEL-ALIM, S. T. BALKE, and A. E. HAMIELEC,
*Department of Chemical Engineering, McMaster University,
Hamilton, Ontario, Canada*

Synopsis

This manuscript reports on the development of a high-shear Couette viscometer. The main design considerations for a high-shear concentric cylinder viscometer are reviewed and discussed. In principle, the instrument is identical to those used by other investigators. However, some modifications were found necessary. Attention is drawn to the importance of the concentricity problem. The instrument was first tested and calibrated using Newtonian standard oils. Then non-Newtonian runs were performed using narrow polystyrene standards of molecular weights 97,200, 411,000, and 860,000. Solutions of the polymer in *n*-butylbenzene ranged in concentration from 0.08 g/cc up to 0.5 g/cc. The shear rates applied ranged from 10^3 sec^{-1} up to 10^6 sec^{-1} . The results obtained were compared to the molecular entanglement theory, and excellent agreement was observed.

INTRODUCTION

The object in designing an instrument to measure flow properties is to obtain "simple shear flow." Analysis of simple shear flow is the most practical route to establishing a constitutive equation because the equations of motion can be solved in terms of the unknown shear stress and rate of deformation tensor components to give a relationship between these unknowns. The results obtained from only one instrument cannot be considered general enough to be a complete constitutive equation since this latter relationship must involve all of the components of the rate of deformation tensor.

Simple shear flow is often obtained by either flow through a capillary (Poiseuille flow), flow between a cone and a plate, or flow between concentric cylinders (Couette flow). All of these instrument types have advantages and disadvantages to a greater or lesser extent depending on their design details.

A high-shear concentric cylinder instrument was a reasonable choice for the work done here. In particular, it has the potential of giving a uniform well-defined shear field and data which require no correction for undesirable effects. Furthermore, the instrument could be based on a design which was proven practical for high shear rates by several investiga-

tors.¹⁻⁶ The original blueprints for our instrument were obtained from Porter.¹

This paper reports a study of the flow behavior of some Newtonian oil standards and of polystyrene solutions in *n*-butylbenzene under high shear field up to 10^5 sec^{-1} .

THE HIGH-SHEAR VISCOMETER

The high-shear viscometer constructed (Fig. 1) is basically the same as that used by Porter,¹ Rechs,⁶ and Barber.⁵ The original blueprints were provided by Porter. The design considerations implemented in the instrument are outlined in the next section.

The apparatus can be considered to consist of the following main components: (1) the thermostating system; (2) the transducing cell, the outer viscometer cylinder, and its mountings; (3) the console containing the electronic controls; and (4) the drive system.

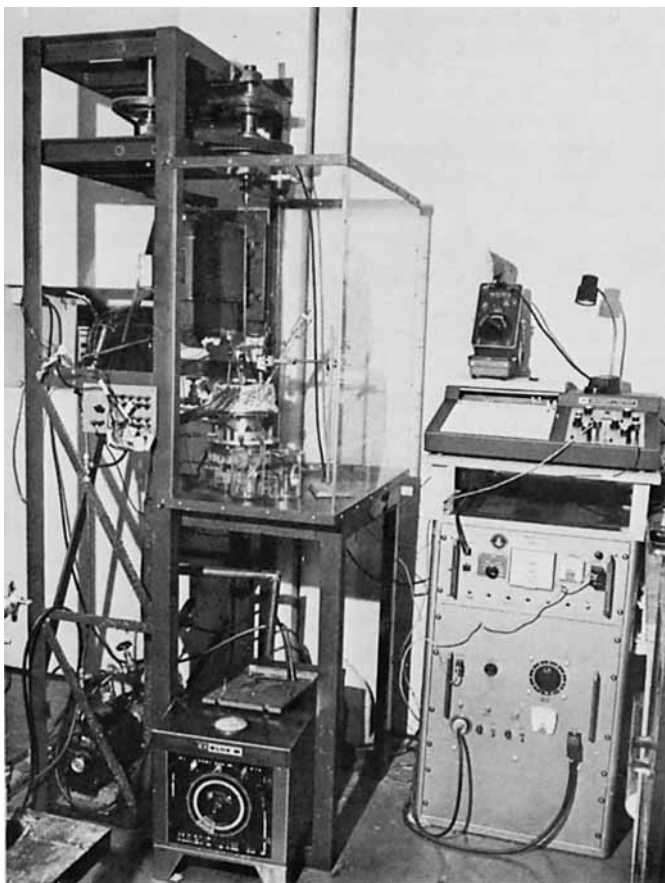


Fig. 1. The high shear viscometer.

The Thermostating System. This system is shown in Figure 1. The bath is a Blue M-Magni Whirl Model MW-1145A-1 Utility Oil Bath. Union Carbide UNCON HTF-30 heat transfer fluid was used. An Albany model gear pump circulated the fluid. Control of flow rate was effected by adjusting the valves in the line. The fluid circulates around the outer cylinder in a brass retaining cup and is prevented from entering the film by a steel guard. Fluid also is sprayed into the inside of the inner rotor.

Viscometer Table and Transducing Cell. The outer cylinder and its attachments are mounted on self-aligning ball bearings. Shear stress is obtained by measuring the force exerted by the torque arm. This measurement is accomplished by positioning a Stratham UC3 transducing cell along the arm at one of seven positions. Two pulleys are mounted opposite each other on needle bearings at the end of the torque arm. They permit calibration of the transducing cell against known weights and accurate positioning of the arm. The transducing cell permits a force in the range of zero to 0.5 lb and zero to 5 lb, depending on the cell adapter used. The power supply used for the cell is very similar to that used by Porter, except that for these cells a 7-volt excitation was required. A range of shear clearances is available by varying the diameter of the inner cylinder. (Details regarding clearances used are given in Table II). Samples were injected by using a glass syringe to the sample inlet tubes.

Electronic Controls. A Sargent two-pen recorder Model DSRG was used to record torque and temperature rpm control was the same as that used by Porter. Measurement of rpm was by stroboscope.

Drive System. A 1 HP Reliance Electric Co. Type T dc motor was used to drive overhead pulleys, which in turn drove a secondary shaft. This secondary shaft held a chuck which attached to the drive semiflexible steel shaft, which was in turn attached to the top of the inner cylinder. Speed control and drive ratio changes were identical to those of Porter.

The following major modifications were found to be necessary: (1) The 1 HP drive motor was mounted on a concrete pillar to reduce vibrations. (Porter's plans had called for this motor to be on the floor.) Rechs also found this modification necessary. (2) The material of construction was changed to Stainless Steel 430. The mild steel originally used corroded very easily. Use of the new material sacrificed some temperature control. (3) The reservoir for coolant fluid was shortened and the fluid guard removed to permit cleaning of the top of the viscometer previous to removing and washing the inner cylinder with solvent for analysis by injection in to the GPC. (The instrument could also be run using continuous feed if necessary to obtain more material for analysis.) For room-temperature runs, the effect of this modification is negligible. For higher-temperature runs, presence of an undesirable axial temperature gradient along the film is possible. Its presence would be indicated by the thermocouple measurements. (4) Using the semiflexible shaft to reduce eccentricity as is shown in the next section.

DESIGN CONSIDERATIONS

Fluid Mechanics

The derivation of the flow equations and the expressions for the shear rate $\dot{\gamma}$ and the shear stress τ are given by Middleman⁷ and Reches⁶:

$$\tau = \frac{Qg_c}{2\pi R^2 L} \quad (1)$$

$$\dot{\gamma} = \frac{2\Omega}{(1 - S^2)} \quad \text{for Newtonian fluids} \quad (2)$$

$$\dot{\gamma} = \frac{2\Omega m}{(1 - S^{2m})} \quad \text{for power-law fluids} \quad (3)$$

Another expression for the shear rate given by Krieger and Elord⁸ was used for the non-Newtonian runs:

$$\dot{\gamma} = \Omega / \ln S (1 + m \ln S) \quad (4)$$

The difference between using eq. (3) and eq. (4) was insignificant since the polymer solutions were almost power-law fluids.

Viscous Heating and Temperature Profiles

Two important aspects result from the viscous heating: (1) the temperature of the film edges, and (2) the maximum temperature rise through the film. Calculation of the first one is relatively easy.⁶ The second one can only be estimated, since it depends on the unknown constitutive equation. However, the use of very small gaps allows for almost a uniform temperature across the gap.⁵ The maximum calculated temperature rise across the gap was about 1°F, and that was considered negligible.

The film temperature cannot be precisely set to a constant value at all shear rates. This is because of the inadequacy of the temperature control system. To obtain data all at one temperature, it is then necessary to find some way of interpolating or extrapolating the result from data obtained at one or more other temperatures.

The Andrades equation is often assumed for the variation of viscosity with temperature:

$$\eta = A \cdot \exp (B/T).$$

For the Newtonian standards, the constants A and B were obtained directly, since the viscosity is given at different temperatures. For the polymer solutions, B was obtained by measuring the viscosity (the efflux time) at different temperatures using more than one capillary viscometer. The results indicate that B is not a function of shear rate (parallel lines on a $\log \eta$ -versus- $1/T$ plot). This was also noticed by Barber et al.⁵

The ratio of the viscosity at a desired temperature T to that at any temperature T_m has been termed the "viscosity factor" and was used to change the shear stress value from T_m to that at the desired temperature T .

End Effects

Shear stress on the ends of the rotating cylinder can ruin the possibilities of good measurement. In this instrument, the film is suspended by surface tension in the annular gap. There is an air-liquid interface above and below the film. This design effectively eliminates end effects.

Concentricity

Concentricity of the inner cylinder in this viscometer is not often considered as a problem in the rheology literature. The problem is not mentioned in previous publications¹⁻⁶ regarding the narrow-gap high-shear concentric cylinder viscometer. The consistently considerable discrepancies between annular gaps measured by micrometer and those calculated by running Newtonian standards in the instrument when very narrow gaps are used were always attributed to the fact that micrometer measurements tended to emphasize high spots on the surface.

Reches⁶ considered the long secondary drive shaft to be a safety device (meant to shear if the inner cylinder seized). He pointed out that it was balanced and periodically checked for alignment. Porter, in a seminar at the University of Toronto, emphasized that the drive shaft was long and thin to provide self-centering by the action of viscous forces in the gap. In a discussion of the Stormer viscometer, a popular rheology text⁹ mentions that two universal joints are supplied in the rotor shaft to permit self-alignment by the action of viscous forces in the narrower portion of the gap but that this sometimes resulted in an undamped pendulum-like motion of the rotor. The only reference quoted by this text on the concentricity problem is the 1939 publication of Inglis.¹⁰ He shows that the torque on the outer cylinder should be multiplied by $(1 - e^2)$, where e is the eccentricity ratio defined as distance between cylinders centers/gap. Clearly, e approaches zero, as the two cylinders are concentric.

Qualitatively speaking, the eccentricity makes the gap wider in one portion than another. This results in a net decrease in fluid transport, a decrease in the average velocity of fluid, and, since the finite velocity of the moving boundary and the zero velocity of the stationary boundary are fixed, an increase in shear rate near the moving boundary and a decrease near the stationary boundary. Thus, shear stress on the stationary boundary is decreased while that on the moving boundary is increased.

Mechanical engineering literature regarding vibration of rotating shafts¹¹ and lubrication of journal bearings¹² offers better understanding. The problem is dealt with by numerically solving the Reynolds equation. The pressure distribution obtained indicates that a film force tends to center the inner cylinder for an absolutely zero-load situation, but that this centering is unstable.¹³

From a polymer rheologist's point of view, the state of the art is unsatisfactory since what progress there has been toward this problem emphasizes the avoidance of actual bearing failure or rough running rather than

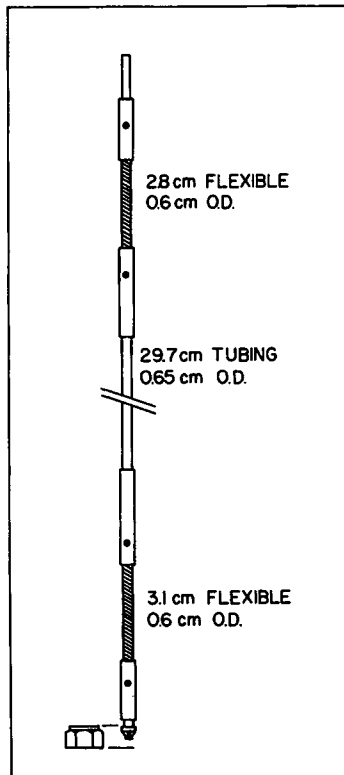


Fig. 2. The semiflexible shaft.

exact prediction of the location of the inner cylinder. The most practical course of action, then, is either to measure eccentricity and involve it as a parameter in the calculations, or to try to eliminate it by proper design.

The second choice was our course of action. After trying several design patterns of the drive shaft,¹⁴ the use of the semiflexible shaft gave a steady, nonvibrating torque recording, indicating concentric operation. Figure 2 shows the shaft used. The central rigid portion is tubular so that unbalance due to material nonhomogeneity is less severe. The flexible end pieces allow for good alignment and provide damping of shaft vibration. The net effect was that the rotational load to the inner cylinder was reduced. The soft iron pins at each end serve as safety measures by shearing if the inner cylinder seized in the outer cylinder.

EXPERIMENTAL AND RESULTS

Details of the experimental procedure are given elsewhere.¹⁴ The instrument was tested and calibrated by standard Newtonian oils (Table I).

Two rotors were used in the study. Dimensions are given in Table II. The rpm was measured directly by a stroboscope. The torque was ob-

TABLE I
Newtonian Standard Oils*

Standard	Viscosity no.
A	S- 3-65-ij
B	S- 20-68-2b
C	S- 200-68-1i
D	S- 2000-68-1e
E	S-30000-67-1g

* Supplied by Cannon Instrument Company, P. O. Box 16, State College, Pa. 16801

TABLE II

Effective Shear Area:	
Length	1.875 in.
Diameter	1.0000 in.
Rotor 1: gap	0.00150 ± 0.00001 in.
Rotor 2: gap	0.00100 ± 0.00001 in.

tained by measuring the force required to maintain the outer cylinder stationary. The transducer cell was calibrated prior to each run.¹⁴

The use of the semiflexible shaft reduced the difference between the micrometer measured gap value and the value calculated from the runs of the Newtonian standards to an acceptable level. Figure 3 shows the results obtained for two different Newtonian standards.

For the non-Newtonian runs, solutions of polystyrene in *n*-butylbenzene were prepared ranging from 0.08 g/cc to 0.5 g/cc. Narrow-polystyrene standards were used, of molecular weights 97,200, 411,000, and 860,000, as shown in Table III. All the results were referred to 30°C as a reference temperature to be compared to the literature.^{15,16}

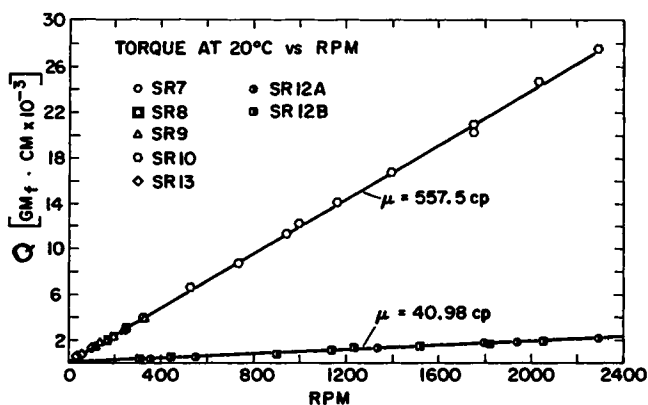


Fig. 3. Torque vs. rpm at 20°C for Newtonian standards B and C. A variety of symbols for data points is used to indicate runs carried out on different days. Two viscosity samples were used.

TABLE III
 Non-Newtonian Runs^a

Run ^b	M	C , g/cc	η_0 , poise	τ_0 , sec $\times 10^3$	τ_r , sec $\times 10^3$
PS1 \times	97,200	0.5	120	1.19	0.56
PS2 \blacktriangle	411,000	0.08	2.2	0.67	0.27
PS3 \triangle	411,000	0.125	5.4	0.89	0.43
PS4 \blacksquare	411,000	0.3	250	12	8.28
PS5 \square	860,000	0.08	8.8	4.16	2.29
PS6 \circ	860,000	0.22	425	43.7	40.18
PS7 \bullet	860,000	0.3	3600	209	249.6

^a Polystyrene standards were supplied by Pressure Chemical Company, 25 Smallman St., Pittsburg, Pa. 15201. They all have polydispersity of less than 1.06.

^b These symbols are used in Figure 6.

Normal stress effects (sample coming out of the gap) were noticed in some cases at very high rpm, but the continuous supply of the feed made that insignificant to the results.

Each run was done by increasing the rpm up to the maximum and then reducing it. This was to check for polymer degradation. The results indicate no degradation since the run followed the same path in both directions. For some runs this was checked further by GPC analysis of the sample before and after shearing; no difference was noticed. Figures 4 and 5 show the results obtained as plots of the apparent viscosity versus shear rate for the runs given in Table III.

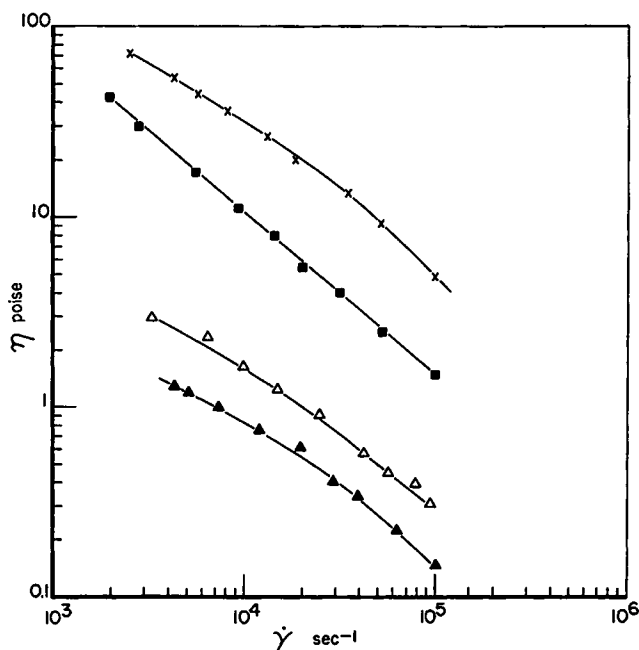


Fig. 4. Viscosity vs. shear rate for runs PS1 to PS4.

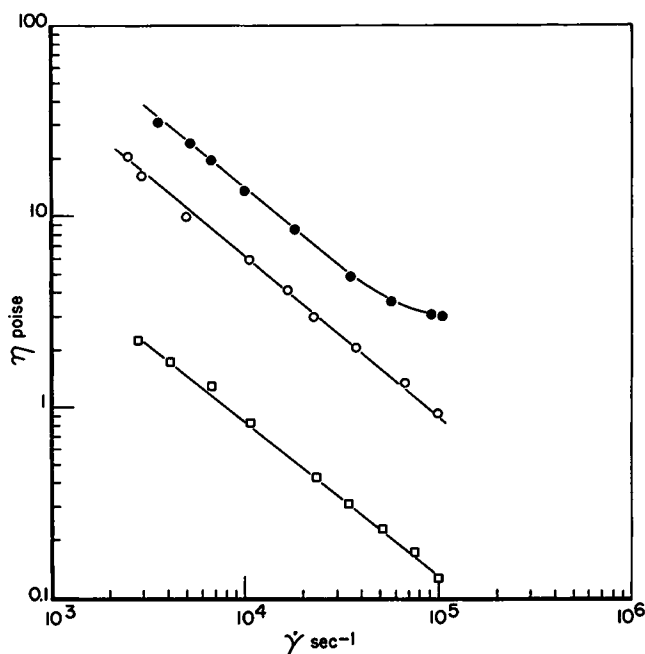


Fig. 5. Viscosity vs. shear rate for runs PS5 to PS7.

The results were analyzed by the method of Graessley.¹⁶ The values of η_0 , the viscosity at zero shear rate, were extracted from the literature¹⁶ since our instrument was not capable of giving data to cover the Newtonian range as well as the non-Newtonian range. Measurements below shear rates of about 10^3 sec^{-1} were not accessible.

In Figure 6, the solid line is the prediction of the entanglement theory of Graessley.¹⁵ The data are shifted horizontally only— η_0 being fixed—to fit the theory. This yields τ_0 , the experimental relaxation time, directly for each sample. Table III shows the observed value of τ_0 as well as the calculated Rouse relaxation time:

$$\tau_r = 6\eta_0 M / \pi^2 CRT.$$

DISCUSSION

It was observed that the data plotted on the dimensionless coordinates show some deviation from the entanglement theory master curve for which the limiting slope is -0.75 . As in Figure 6, the data show a limiting slope of -0.83 . The drop of η/η_0 with $\gamma \tau_0/2$ is thus steeper than predicted. This was also observed by Graessley et al.¹⁶ Many theories have been proposed to predict non-Newtonian viscosity.⁷ Bueche^{17,18} assumed that the polymer molecule rotates owing to solvent flow and is subjected accordingly to periodic deformation. This theory yields a limiting slope of -0.5 , which is less than what was noticed experimentally. Graessley¹⁵

developed a theory based on the concept of molecular entanglement. The basic idea of this theory is that for an entanglement to exist, two molecules must be within a certain distance of each other and remain as such for a finite time τ , or else no entanglement occurs. At higher shear rates, chances of these two conditions to be fulfilled are slim. Hence, the entanglement density is reduced by high shear rate resulting in a drop of viscosity.

Again, this theory predicts a limiting slope of -0.75 . Williams¹⁹ proposed a theory which makes no commitment to a specific mechanism of interaction between molecules. His theory predicts a limiting slope of -1.0 . The present study indicates a limiting slope of -0.83 , which is quite close to that observed by Stratton.²⁰ His work on polystyrene

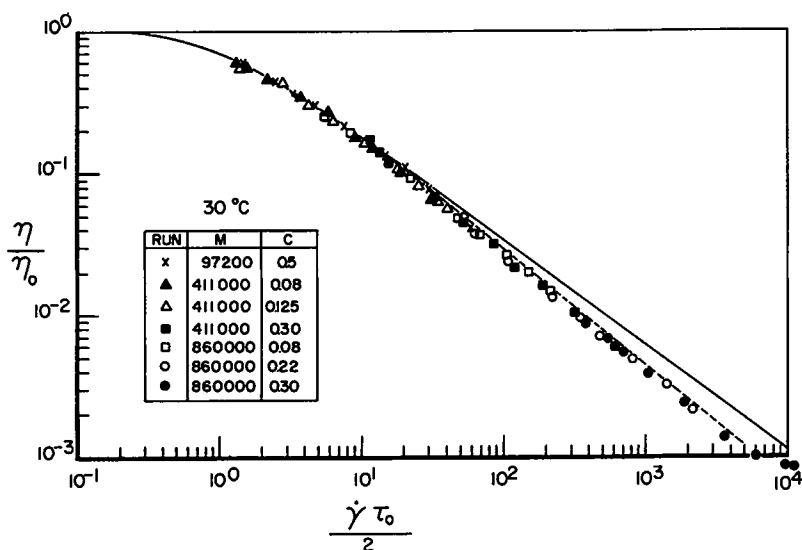


Fig. 6. Reduced viscosity vs. reduced shear rate for the different runs; solid line is the original entanglement theory; dashed line is the modified theory.

melts using a capillary rheometer shows a limiting slope of -0.82 . He noticed that at high shear rates, the viscosity is not a function of molecular weight. This was observed in the present study, as shown in Figures 4 and 5; runs of the same concentration and different molecular weights show almost the same viscosity. Stratton postulated that the decrease in viscosity with increasing shear rate is due to an increase in the spacing of coupling entanglements.²⁰

Graessley,²¹ then, modified his theory. The modified theory predicts a limiting slope of -0.818 with which the present results agree very well.

At about $\gamma \tau_0/2$ of 10^4 , there seems to be some leveling of the curve. This was noticed in run PS7 of the highest molecular weight. Unfortunately, only this run could reach $\gamma \tau_0/2$ of 10^4 . Further work at higher shear rates is needed before any conclusions can be made.

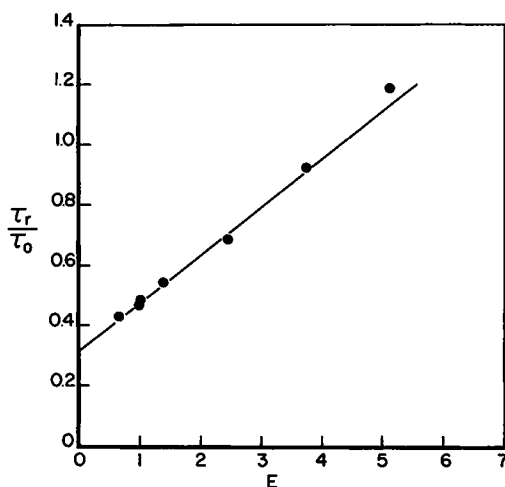


Fig. 7. Plot of τ_r/τ_0 vs. entanglement density.

Values of τ_r/τ_0 were plotted versus the entanglement density E , defined for this system by Graessley as

$$E = CM/(CM_b) = CM/50,500$$

where CM_b is the break point on the plot of η_0 versus M for different concentrations.¹⁶

Such a plot is shown in Figure 7. The best straight line fit yields the relationship

$$\tau_r/\tau_0 = 0.32 + 0.16E = 0.32 (1 + 0.5E)$$

which indicates a lower slope and a higher intercept than those given by Graessley et al.¹⁶

$$\tau_r/\tau_0 = 0.28 (1 + 0.67E).$$

Nomenclature

- τ shear stress
- Q torque
- R radius of rotor
- L length of the common cylindrical area between the two cylinders
- Ω rpm
- γ shear rate
- S ratio between the radius of the inner cylinder to that of the outer cylinder
- m slope of the curve $\log \Omega$ vs. $\log Q$ ($m = d \log \Omega / d \log Q$)
- η viscosity
- η_0 viscosity at zero shear rate
- T absolute temperature
- τ_r Rouse relaxation time

- τ_0 observed relaxation time
 M molecular weight
 C solution concentration
 E entanglement density

References

1. R. S. Porter and J. F. Johnson, *J. Phys. Chem.*, **63**, 202 (1959).
2. R. S. Porter, and J. F. Johnson, *J. Appl. Phys.*, **35**, 3149 (1964).
3. R. S. Porter, R. F. Klaver, and J. F. Johnson, *Rev. Sci. Instr.*, **36**, 1846 (1965).
4. R. S. Porter, J. F. Johnson, and M. J. R. Cantow, *J. Polym. Sci.*, **16**, 1 (1967).
5. E. M. Barber, J. R. Muenger, and F. J. Villforth, *Anal. Chem.*, **27**, 3 (1955).
6. E. Reches, Ph.D. Thesis, University of Cincinnati, 1967.
7. S. Middleman, *The Flow of High Polymers*, Interscience, New York, 1968.
8. I. M. Krieger, and H. Elord, *J. Appl. Phys.*, **24**(No. 2), 134 (1953).
9. J. R. Van Wazer, J. W. Lyons, K. Y. Kim, and R. E. Colwell, *Viscosity and Flow Measurement*, Interscience, New York, 1963.
10. D. R. Inglis, *Phys. Rev.*, **56**, 1041 (1939).
11. R. E. D. Bishop, and A. G. Parkinson, *Appl. Mech. Rev.*, **21**, 439 (1968).
12. A. Cameron, *The Principles of Lubrication*, Wiley, New York, 1966.
13. Y. Hori, *J. Appl. Mech.*, *Trans. of ASME*, 189 (1959).
14. S. T. Balke, Ph.D. Thesis, McMaster University, 1972.
15. W. W. Graessley, *J. Chem. Phys.*, **43**(8), 2696 (1965).
16. W. W. Graessley, R. L. Hazleton, and L. R. Lindeman, *Trans. Soc. Rheol.*, **11**(3), 267 (1967).
17. F. Bueche, *Physical Properties of Polymers*, Interscience, New York, 1965, p. 308.
18. F. Bueche, *J. Chem. Phys.*, **22**, 1570 (1954).
19. M. C. Williams, *A.I.Ch.E.J.*, **12**, 1064 (1966).
20. R. A. Stratton, *J. Colloid Interfac. Sci.*, **22**, 517 (1966).
21. W. W. Graessley, *J. Chem. Phys.*, **47**(6), 1942 (1967).

Received September 1972